LUNAR MANTLE TEMPERATURE STRUCTURE FROM SEISMIC AND GEODETIC OBSERVATIONS AND LABORATORY DISSIPATION EXPERIMENTS. F. Nimmo, *Dept. Earth & Planetary Sciences, U.C. Santa Cruz, Santa Cruz CA 95064 (fnimmo@es.ucsc.edu)*, U. Faul, *Dept. Earth Sciences, Boston University, Boston MA 02215 (ufaul@bu.edu)*.

Summary We model the temperature and rigidity structure of the Moon using constraints provided by laboratory experiments on olivine aggregates. Our best-fit model matches the measured dissipation factor Q at both tidal and seismic frequencies, and reproduces the measured k_2 tidal Love number. In this model, two-thirds of the heat-producing elements are in the crust, and the lunar mantle is relatively cold. A deep zone of partial melting is not required to explain either Q or k_2.

Introduction The temperature structure of the Moon informs us about its thermal evolution and controls the mechanical properties of its interior. Mechanical properties such as rigidity and the degree of dissipation are constrained by seismic [1] and geodetic [2] observations. Laboratory experiments provide the missing link, allowing the influence of temperature on rigidity and dissipation to be measured [3,4]. Dissipation is very sensitive to temperature variations, while rigidity and seismic velocity are more sensitive to mineralogy. Although various studies of the lunar interior based primarily on seismic data have been carried out [5-8], in general these have not used laboratory dissipation experiments as a constraint.

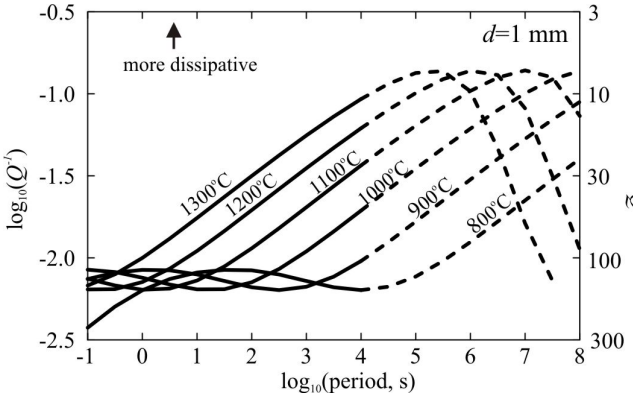

Figure 1: Predicted dissipation factor Q^{-1} as a function of temperature and period for melt-free olivine aggregates, based on laboratory experiments and assuming a grain size of 1 mm. Calculations were carried out using the extended Burgers model of [3], using the rheological parameters given in their Table 2. Dashed lines denote approximate region of extrapolation beyond the experimentally-derived values.

Observations The bulk Q of the Moon at tidal frequencies has been measured by lunar laser ranging (LLR) [2,9], while the tidal Love number k_2 has been inferred from both gravity [10] and LLR studies [2,9]. At seismic frequencies, dissipation increases (Q decreases) with depth [5-7], while it has been argued that the deep mantle may contain a layer of partial melt [5]. The S-wave velocity is approximately constant [5,6], except near the surface and possibly near the CMB [5]. The frequency-dependence of Q in the upper mantle is weak [11], while the bulk tidal Q is almost frequency-independent [9].

Laboratory Experiments Laboratory experiments have documented how rock elastic moduli and dissipation factor Q vary with temperature, frequency and grain size [3,4]. As with seismic observations [11], the lab-derived frequency-dependence of Q shows that a simple Maxwell viscoelastic description is inadequate, and that more complicated descriptions such as the Andrade or Burgers model are required [3]. Figure 1 shows how Q^{-1} is predicted to vary with frequency and temperature for a melt-free olivine aggregate, using the experimentally-derived modified Burgers model of [3]. Similar models have successfully reproduced the seismic behaviour of the shallow terrestrial mantle, without requiring the presence of melt or fluids [12]. At short periods, Fig 1 shows that there is a temperature interval over which Q ($\approx$200) is approximately independent of both temperature and frequency. Dissipation increases at longer periods, with the period at which peak dissipation occurs increasing with decreasing temperature. Note that the location of the peak is only weakly constrained by the experimental observations.

Model For a given temperature and deformation period, the complex rigidity and seismic velocities may be calculated using the approach exemplified by Figure 1. Given a complex rigidity structure, global properties such as Q and the tidal Love numbers h_2, k_2 may then be calculated, assuming spherical symmetry [13]. The density structure used here is a simple two-layer model, in which the core has a radius of 350 km [5] and density of 7 g/cc and the mantle has an outer radius of 1740 km and a density at zero pressure of 3.3 g/cc. The variation in mantle density with depth is calculated assuming a bulk modulus of 140 GPa and a gravitational acceleration that varies linearly with radius. The temperature structure is calculated assuming steady-state heat conduction with zero heat flux at the CMB and two heat-producing layers. The total heat production is assumed to be 0.48 TW based on deductions of the Moon's radiogenic element concentrations [14], and the upper layer (crust) is assumed to have a thickness of 45 km. The complex rigidity is calculated in the same fashion as for Fig 1, assuming a 1 mm grain-size.

Results The red line in Figure 2a shows the resulting temperature structure with crustal and mantle heat production rates of 180 and 8.5 $\mathrm{nW\ m^{-3}}$, respectively, such that two-thirds of heat production occurs in the crust. This may be compared with the shaded regions, which denote the *a posteriori* temperature probability distribution derived by [8] primarily from inversion of seismic data. The match is reasonable, except in the uppermost 400 km, where our temperatures are systematically colder than those of [8]. The blue lines denote model and inferred seismic Q, respectively. At shallow depths, our model overestimates Q, because it does not take scattering into account. In the deepest mantle, our model is too dissipative,

by a factor ≈2. The green lines show model and inferred S-wave velocities. Deep-mantle values are in good agreement, but the model shallow values are too low, probably because of our simplified mineralogical model.

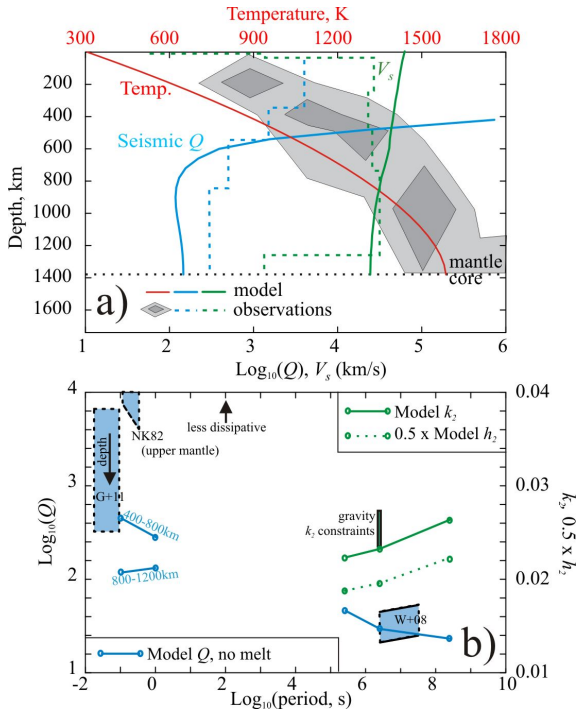

Figure 2: a) Model temperature structure and resulting dissipation factor Q and S-wave velocity V_s within the Moon. Temperature structure is derived by assuming steady-state conduction in which the 45 km thick crust and 1345 km thick mantle are heated at rates of 180 and 8.5 $\mathrm{nW\ m^{-3}}$, respectively. The shaded regions denote the *a posteriori* lunar temperature probability distribution, from joint inversion of multiple data sets [8]. The model Q at 10 Hz is compared with the seismically-derived Q structure from [6]. The model V_s is compared with the seismically-derived values from [5]. b) Comparison of model and observed Q and k_2. Seismic constraints are from [6] and [11]. Tidal constraints on Q are from [9], and tidal constraints on k_2 are from [10]. In general the model results match the observations quite well.

Figure 2b compares the model and observed Q, k_2 and h_2 as a function of frequency. At monthly periods we obtain values for Q,k_2 and h_2 of 30, 0.0233 and 0.0392, respectively. The model Q at tidal frequencies shows only a weak frequency dependence and agrees with constraints derived from LLR [9]. The model k_2 at these frequencies agrees with the constraints derived from LLR ($k_2 = 0.0229 \pm 0.0020$ [2]) and is at the bottom of the range derived from satellite tracking ($k_2 = 0.0255 \pm 0.0016$ [10]). At seismic frequencies, the inferred upper-mantle frequency-dependence of Q [11] is approximately reproduced, but the model dissipation is somewhat higher than that observed. The predicted mid-mantle frequency-dependence of Q is very small.

Because of its strong temperature-dependence at long periods, Q is a good probe of temperature structure. Furthermore, there is a tradeoff between Q and k_2: for instance, reducing the deep mantle temperature slightly improves the fit to the seismic Q values, but increases the misfit to k_2 (because of the increased mantle rigidity). Moving radiogenic elements from crust to mantle results in a hotter mantle and a Moon that is too dissipative. Conversely, the effect of grain size is small: increasing it by an order of magnitude increases the tidal Q by a factor of 2 and reduces k_2 by 8%.

Discussion and Conclusions The preliminary results shown in Fig 2 demonstrate that a physically reasonable temperature structure can broadly reproduce the seismic and tidal characteristics of the Moon, without requiring additional mechanisms such as melting. This is because olivine aggregates (and, by assumption, planetary mantles) are quite dissipative at long periods even when melt-free (Fig 1, [3,12]). If additional dissipation mechanisms (such as partial melting) are present, then the background temperature structure of the Moon must be even colder than shown in Fig 2.

Our results are unlikely to be affected by likely variations in grain size. The presence of solid secondary phases is expected to have an insignificant effect on Q; such phases will likely have a larger effect on V_s [8], which may explain some of the observed mismatch in the shallow mantle.

Fig 2 suggests that a large fraction of the Moon's radiogenic elements are sequestered in the crust.Our heat flow model is undoubtedly oversimplified, and needs further investigation. Nonetheless, the crustal heating rate ($180\ \mathrm{nW\ m^{-3}}$) assumed here agrees well with the surface heating rate of ($160\ \mathrm{nW\ m^{-3}}$) derived from the observed 1 ppm surface Th concentrations [14].

Further modelling involving more realistic mineralogies is required to reduce the mismatch observed for the near-surface seismic values of Q and V_s. Acquisition of more accurate observations by the GRAIL mission will allow tighter constraints to be placed on the temperature structure. The analysis presented here may also be applicable to other bodies where tidal Q has been measured, such as Mars [15].

References

[1] Lognonne, P., C. Johnson, Treat. Geophys. 10, 69-116, 2007. [2] Williams, J.G. et al., JGR 106, 27933-68, 2001. [3] Jackson, I., U.H. Faul, PEPI 183, 151-163, 2010. [4] Gribb, T.T., R.F. Cooper, JGR 103, 27267-79, 1998. [5] Weber, R.C. et al., Science 331, 309-312, 2011. [6] Garcia, R.F. et al., PEPI 188, 96-113, 2011. [7] Lognonne, P., B. Mosser, Surv. Geophys. 14, 239-302, 1993. [8] Khan A. et al., JGR 111, E05005, 2006. [9] Williams, J.G. et al., Proc. 16th Int. Workshop. Laser Ranging, Poznan, Poland, 2009. [10] Goossens, S. et al., J. Geod. 85, 205-228, 2011. [11] Nakamura, Y., J. Koyama, JGR 87, 4855-61, 1982. [12] Faul, U.H., I. Jackson, EPSL 234, 119-134, 2005. [13] Roberts, J.H., F. Nimmo, Icarus 194, 675-689, 2008. [14] Garrick-Bethell, I. et al., Science 330, 949-951, 2010. [15] Bills, B.G. et al., JGR 110, E07004, 2005.